Contact Representations of Graphs in 3D

J. Alam[1], W. Evans[2], S. Kobourov[1], S. Pupyrev[1,3], J. Toeniskoetter[1], and T. Ueckerdt[4]

[1] Department of Computer Science, University of Arizona, USA
[2] Department of Computer Science, University of British Columbia, Canada
[3] Institute of Mathematics and Computer Science, Ural Federal University, Russia
[4] Department of Mathematics, Karlsruhe Institute of Technology, Germany

Abstract. We study contact representations of non-planar graphs in which vertices are represented by axis-aligned polyhedra in 3D and edges are realized by non-zero area common boundaries between corresponding polyhedra. We present a liner-time algorithm constructing a representation of a 3-connected planar graph, its dual, and the vertex-face incidence graph with 3D boxes. We then investigate contact representations of 1-planar graphs. We first prove that optimal 1-planar graphs without separating 4-cycles admit a contact representation with 3D boxes. However, since not every optimal 1-planar graph can be represented in this way, we also consider contact representations with the next simplest axis-aligned 3D object, L-shaped polyhedra. We provide a quadratic-time algorithm for representing optimal 1-planar graphs with L-shapes.

1 Introduction

Graphs are often used to describe relationships between objects, and graph embedding techniques allow us to visualize such relationships. There are compelling theoretical and practical reasons to study *contact representations* of graphs, where vertices are interior-disjoint geometric objects and edges correspond to pairs of objects touching in some specified fashion. In practice, 2D contact representations with rectangles, circles, and polygons of low complexity are intuitive, as they provide the viewer with the familiar metaphor of geographical maps. Such representations are preferred in some contexts over the standard node-link representations for displaying relational information [9].

A large body of work considers representing graphs by contacts of simple curves or polygons in 2D. Graphs that can be represented in this way are planar and Koebe's 1936 theorem established that *all* planar graphs can be represented by touching disks [18]. Every planar graph also has a contact representation with triangles [15]. Curves, line-segments, and L-shapes have also been used [14, 17]. In particular, it is known that all planar bipartite graphs can be represented by contacts of axis-aligned segments [10]. For non-planar graphs such contact representations in 2D are impossible. In a natural generalization for non-planar graphs, vertices can be represented with 3D-polyhedra. For example, representations of complete graphs and complete bipartite graphs using spheres and cylinders have been considered [5, 16]. Overall, very little is known about such contact representations of non-planar graphs.

As a first step towards representing non-planar graphs, we consider *primal-dual* contact representations, in which a plane graph (a planar graph with a fixed planar em-
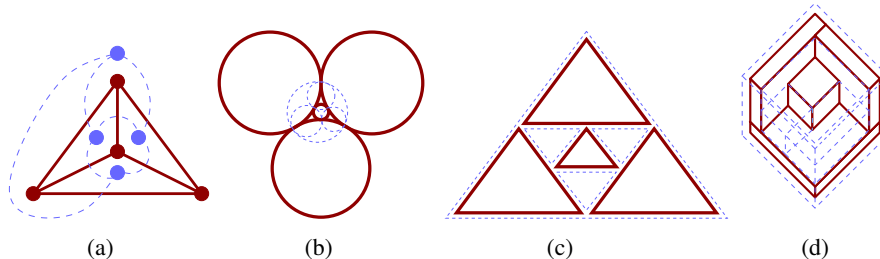
Fig. 1: (a) A plane graph K_4 and its dual; primal-dual contact representations of the graph with (b) circles and (c) triangles. (d) The primal-dual box-contact representation of K_4 with dual vertices shown dashed. The outer box (shell) contains all other boxes.

bedding), its dual graph, and the face-vertex incidence graph are all represented simultaneously. More formally, in such a representation vertices and faces are represented by some geometric objects so that:

(i) the objects for the vertices are interior-disjoint and induce a contact representation for the primal graph;

(ii) the objects for the faces are interior-disjoint except for the object for the outer face, which contains all the objects for the internal faces, and together they induce a contact representation of the dual graph;

(iii) the objects for a vertex v and a face f intersect if and only if v and f are incident.

Primal-dual representations of plane graphs have been studied in 2D. Every 3-connected plane graph has a primal-dual representation with circles [2] and triangles [15]; see Fig. 1(a)–(c). Our first result in this paper is an analogous primal-dual representation using axis-aligned 3D boxes. While it is known that every planar graph has a contact representation with 3D boxes [7, 12, 23], Theorem 1 strengthens the result; see Fig. 1d.

Theorem 1. *Every 3-connected plane graph $G = (V, E)$ admits a proper primal-dual box-contact representation in 3D and it can be computed in $\mathcal{O}(|V|)$ time.*

Before proving this theorem we point out two important differences between our result for box-contact representation and the earlier primal-dual representations for circles and triangles [2, 15]. First, the existing constructions induce *non-proper* (point) contacts, while our contacts are always *proper*, that is, have non-zero areas. Second, for a given 3-connected plane graph, it is not always possible to find a primal-dual representation with circles by a polynomial-time algorithm, although it can be constructed numerically by polynomial-time iterative schemes [19]. There is also no known polynomial-time algorithm that computes a primal-dual representation with triangles for a given plane graph. In contrast, our box-contact representation for an n-vertex graph can be computed in linear time and realized on the $\mathcal{O}(n) \times \mathcal{O}(n) \times \mathcal{O}(n)$ grid.

We prove Theorem 1 with a constructive algorithm, which uses the notions of Schnyder woods and orthogonal surfaces, as defined in [13]. It is known that every 3-connected planar graph induces an orthogonal surface; we will show how to construct a new contact representation with interior-disjoint boxes from such an orthogonal sur-

2

face. Since the orthogonal surfaces for a 3-connected planar graph and its dual coincide *topologically*, we show how to *geometrically* realize the primal and the dual box-contact representations so that they fit together to realize all the desired contacts. The construction idea is inspired by recent box-contact representation algorithms for maximal planar graphs [7]. Note, however, that we generalize one such algorithm to handle 3-connected planar graphs (rather than maximal-planar graphs) and show how to combine the primal and dual representations. Our method relies on a correspondence between Schnyder woods and generalized canonical orders for 3-connected planar graphs. Although the correspondence has been claimed in [3], the earlier proof appears to be incomplete. We provide a complete proof of the claim in the full version of the paper [1].

The representation in Theorem 1 immediately gives box-contact representations for a special class of non-planar graphs that are formed by the union of a planar graph, its dual, and the vertex-face incidence graph. The graphs were called *prime* by Ringel [20], who studied them in the context of simultaneously coloring a planar graph and its dual, and are defined as follows. A simple graph $G = (V, E)$ is said to be 1-*planar* if it can be drawn on the plane so that each of its edges crosses at most one other edge. A 1-planar graph has at most $4|V| - 8$ edges and it is *optimal* if it has exactly $4|V| - 8$ edges [11], that is, it is the densest 1-planar graph on the vertex set. An optimal 1-planar graph is called *prime* if it has no separating 4-cycles, that is, cycles of length 4 whose removal disconnects the graph. These optimal 1-planar graphs are exactly the ones that are 5-connected; alternatively, these graphs can be obtained as the union of a 3-connected simple plane graph, its dual and its vertex-face-incidence graph [21].

As in earlier primal-dual contact representations, it is not possible to have all vertex-objects interior disjoint. Specifically, one vertex-object (be it triangle, circle, or box) contains all the others. We call this special box the *shell* and such a representation a *shelled* box-contact representation. Here all the vertices are represented by 3D boxes, except for one vertex, which is a shell, and the interiors of all boxes and the exterior of the shell are disjoint. Note that a similar shell is required in circle-contact and triangle-contact representations; see Fig. 1. The following is a direct corollary of Theorem 1.

Corollary 1. *Every prime 1-planar graph G has a shelled box-contact representation in 3D and it can be computed in linear time.*

Fig. 2: An L-shaped polyhedron.

One may wonder whether every 1-planar graph admits a box-contact representation in 3D, but it is easy to see that there are 1-planar graphs, even as simple as K_5, that do not admit a box-contact representation. Furthermore, there exist optimal 1-planar graphs (which contain separating 4-cycles) that have neither a box-contact representation nor a shelled box-contact representation; see the full paper [1].

Therefore, we consider representations with the next simplest axis-aligned object in 3D, an L-shaped polyhedron or simply an $\mathcal{L}$, which is an axis-aligned box minus the intersection of two axis-aligned half-spaces; see Fig. 2. An $\mathcal{L}$ can also be considered the union of two 3D boxes. Note that the union of two axis-aligned boxes does not always form an $\mathcal{L}$ (e.g., it could form a T-shape); an $\mathcal{L}$ is the simplest of all such polyhedra. We provide a quadratic-time algorithm for representing every optimal 1-planar graph with $\mathcal{L}$'s (note that a 3D box is simply a degenerate $\mathcal{L}$).
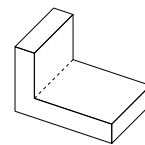
Theorem 2. *Every embedded optimal* 1-*planar graph* $G = (V, E)$ *has a proper* $\mathcal{L}$-*contact representation in 3D and it can be computed in* $\mathcal{O}(|V|^2)$ *time.*

Our algorithm is similar to a recursive procedure used for constructing box-contact representations of planar graphs in [12, 23]. The basic idea is to find separating 4-cycles and represent the inner and the outer parts of the graph induced by the cycles separately. Then these parts are combined to produce the final representation. Since the separating 4-cycles can be nested inside each other, the running time of our algorithm is dominated by the time required to find separating 4-cycles and their nested structure. Unlike the early algorithms for box-contact representations of planar graphs [12, 23], our algorithms produce proper contacts between the 3D objects (boxes and $\mathcal{L}$'s).

2 Primal-Dual Representations of 3-Connected Plane Graphs

In this section we prove Theorem 1. Specifically, we describe a linear-time algorithm that computes a box-contact representation for the primal graph and the dual graph separately and then fits them together to also realize the face-vertex incidence graph. We first require some concepts about Schnyder woods and ordered path partitions.

Let G be a 3-connected plane graph with a specified pair of vertices $\{v_1, v_2\}$ and a third vertex $v_3 \notin \{v_1, v_2\}$, such that v_1, v_2, v_3 are all on the outer face in that counterclockwise order. Add the edge (v_1, v_2) to the outer face of G (if it does not already contain it) such that v_3 remains on the outerface and call the augmented graph G'. Let $\Pi = (V_1, V_2, \ldots, V_L)$ be a partition of the vertices of G such that each V_i induces a path in G; Π is an *ordered path partition* [3] of G if the following conditions hold:
(1) V_1 contains the vertices on the counterclockwise path from v_1 to v_2 on the outer cycle; $V_L = \{v_3\}$;
(2) for $1 \leq k \leq L$, the subgraph G_k of G' induced by the vertices in $V_1 \cup \ldots \cup V_k$ is 2-connected and internally 3-connected (that is, removing two internal vertices of G_k does not disconnect it); hence the outer cycle C_k of G_k is a simple cycle containing the edge (v_1, v_2);
(3) for $2 \leq k \leq L$, each vertex on C_{k-1} has at most one neighbor in V_k.

The pair (v_1, v_2) forms the *base-pair* for Π and v_3 is the *head vertex* of Π. For an ordered path partition $\Pi = (V_1, V_2, \ldots, V_L)$ of G, a vertex v of G has *label* k if $v \in V_k$. The *predecessors* of v are the neighbors of v with equal or smaller labels; the *successors* of v are the neighbors of v with equal or larger labels; see Fig. 3a.

Again consider the three specified vertices v_1, v_2, v_3 in that counterclockwise order on the outer face of G. For $i \in \{1, 2, 3\}$, add a half-edge from v_i reaching into the outer face. A *Schnyder wood* [6] is an orientation and a coloring of the edges of G (including the added half-edges) with the colors $1, 2, 3$ satisfying the following conditions:
(1) every edge e is oriented in either one (*uni-directional*) or two opposite directions (*bi-directional*). The edges are colored so that if e is bi-directional, the two directions (half-edges) have distinct colors;
(2) the half-edge at v_i is directed outwards and colored i;
(3) each vertex v has out-degree exactly one in each color, and the counterclockwise order of edges incident to v is: outgoing in color 1, incoming in color 2, outgoing in color 3, incoming in color 1, outgoing in color 2, incoming in color 3;

4
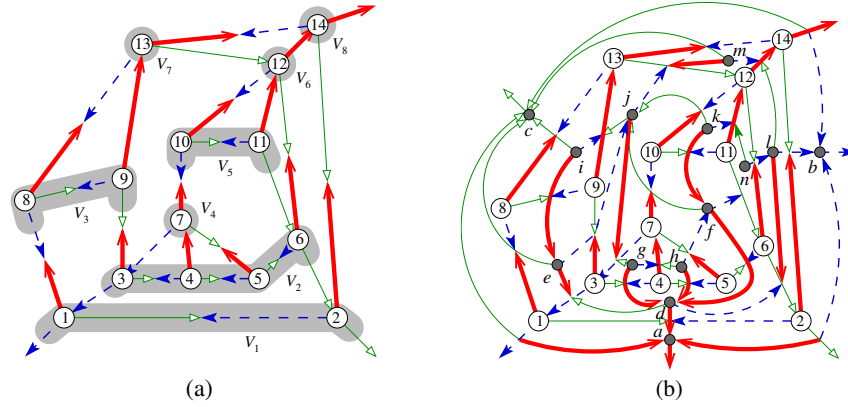
Fig. 3: (a) An ordered path partition and its corresponding Schnyder wood for a 3-connected graph G. (b) The Schnyder woods for the primal and the dual of G. The thick solid red, dotted blue and thin solid green edges represent the three trees in the Schnyder wood.

(4) there is no interior face whose boundary is a directed cycle in one color.

These conditions imply that for $i \in \{1, 2, 3\}$, the edges with color i induce a tree $\mathcal{T}_i$ rooted at v_i, where all edges of $\mathcal{T}_i$ are directed towards the root. Denote by $\mathcal{T}_i^{-1}$ the tree with all the edges of $\mathcal{T}_i$ reversed, and the Schnyder wood by $(\mathcal{T}_1, \mathcal{T}_2, \mathcal{T}_3)$. Every 3-connected plane graph has a Schnyder wood [4, 13]. From a Schnyder wood of a 3-connected plane graph G, one can construct a *dual Schnyder wood* (the Schnyder wood for the dual of G). Consider the dual graph G^* of G in which the vertex for the outer face of G has been split into three vertices forming a triangle. These three vertices represent the three regions between pairs of half edges from the outer vertices of G. Then a Schnyder wood for G^* is formed by orienting and coloring the edges so that between an edge e in G and its dual e^* in G^*, all three colors $1, 2, 3$ have been used. In particular, if e is uni-directional in color i, $i \in \{1, 2, 3\}$, then e^* is bi-directional in colors $i - 1, i + 1$ and vice versa; see Fig. 3b; also see [6].

It is known that an ordered path partition of G defines a Schnyder wood on G, where the three outgoing edges for each vertex are to its (1) leftmost predecessor, (2) right-most predecessor, and (3) highest-labeled successor [4, 13]. We call an ordered path partition and the corresponding Schnyder wood computed this way to be *compatible* with each other. Badent et al. [3] argue that the converse can also be done, that is, given a Schnyder wood on G, one can compute an ordered path partition, compatible with the Schnyder wood (and hence, there is a one-to-one correspondence between the concepts). However, the algorithm in [3] for converting a Schnyder wood to a compatible ordered path partition is incomplete, that is, the computed ordered path partition is not always compatible with the Schnyder wood. In the full version of the paper [1] we show such an example and provide a correction of the algorithm. Hence, we have:

Lemma 1. *Let $(\mathcal{T}_1, \mathcal{T}_2, \mathcal{T}_3)$ be a Schnyder wood of a 3-connected plane graph G with three specified vertices v_1, v_2, v_3 in that counterclockwise order on the outer face. Then for $i \in \{1, 2, 3\}$, one can compute in linear time an ordered path partition Π_i*

5
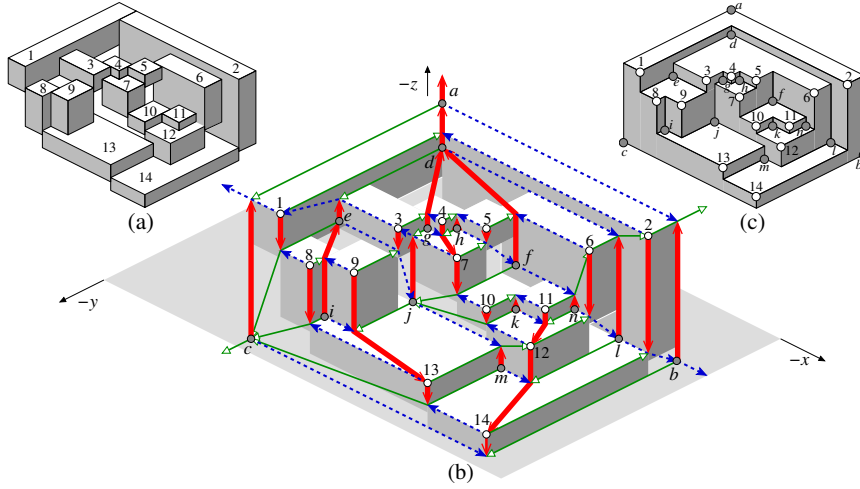
Fig. 4: Box-contact representation (a) for the graph in Fig. 3 with its primal-dual Schnyder wood (b) and the associated orthogonal surface (c). The thick solid red, dotted blue and thin solid green edges represent the three trees in the Schnyder wood.

compatible with $(\mathcal{T}_1, \mathcal{T}_2, \mathcal{T}_3)$ such that Π_i has (v_{i-1}, v_{i+1}) as the base-pair and v_i as the head. Furthermore Π_i is consistent with the partial order defined by $\mathcal{T}_{i-1}^{-1} \cup \mathcal{T}_{i+1}^{-1} \cup \mathcal{T}_i$.

We denote a connected region in a plane embedding of a graph by a *face*, and a side of a 3D shape by a *facet*. For a 3D box R, call the facet with highest (lowest) x-coordinate as the x^+-facet (x^--facet) of R. The y^+-facet, y^--facet, z^+-facet and z^--facet of R are defined similarly. For convenience, we denote the x^+-, x^--, y^+-, y^--, z^+- and z^--facets of R as the *right*, *left*, *front*, *back*, *top* and *bottom* facets of R, respectively. We now sketch a proof for Theorem 1; see [1] for a complete version.

Theorem 1. *Every 3-connected plane graph $G = (V, E)$ admits a proper primal-dual box-contact representation in 3D and it can be computed in $\mathcal{O}(|V|)$ time.*

Proof sketch. Our algorithm consists of the following steps. Let v_1, v_2 and v_3 be three vertices on the outer face of G in the counterclockwise order. First, we create a Schnyder wood $(\mathcal{T}_1, \mathcal{T}_2, \mathcal{T}_3)$ such that for $i \in \{1, 2, 3\}$, $\mathcal{T}_i$ is rooted at v_i. Then using Lemma 1, we compute three ordered path partitions compatible with $(\mathcal{T}_1, \mathcal{T}_2, \mathcal{T}_3)$. Next the ordered path partitions are used to calculate the coordinates of 3D boxes that form a contact representation for the primal graph G; a number of local modifications is performed to obtain proper contacts. Finally, the same steps are applied, starting with the dual Schnyder wood of $(\mathcal{T}_1, \mathcal{T}_2, \mathcal{T}_3)$, to construct the representation of the dual graph G^*. These two representations induce the same orthogonal surfaces [13]; hence, they can be combined together to form a primal-dual box-contact representation.

Note that a similar idea is used in [7] to compute a box-contact representation for a maximal planar graph. We strengthen the result by (1) generalizing the method to 3-connected planar graphs and (2) computing an ordered path partition compatible with a Schnyder wood. The latter guarantees the fit between the primal and the dual.

We sketch the steps for computing the primal representation from a Schnyder wood $(\mathcal{T}_1, \mathcal{T}_2, \mathcal{T}_3)$; the computation for the dual representation is analogous. By Lemma 1, for $i \in \{1, 2, 3\}$, one can compute a compatible ordered path partition with the base-pair (v_{i-1}, v_{i+1}) and head v_i, consistent with the partial order defined by $\mathcal{T}_{i-1}^{-1} \cup \mathcal{T}_{i+1}^{-1} \cup \mathcal{T}_i$. Denote by $<_X$, $<_Y$ and $<_Z$ the three ordered path partitions compatible with $(\mathcal{T}_1, \mathcal{T}_2, \mathcal{T}_3)$, that are consistent with $\mathcal{T}_3^{-1} \cup \mathcal{T}_2^{-1} \cup \mathcal{T}_1$, $\mathcal{T}_1^{-1} \cup \mathcal{T}_3^{-1} \cup \mathcal{T}_2$, and $\mathcal{T}_2^{-1} \cup \mathcal{T}_1^{-1} \cup \mathcal{T}_3$, respectively. For a vertex u, let $x_M(u)$, $y_M(u)$, and $z_M(u)$ be the labels of u in the ordered path partitions $<_X$, $<_Y$, and $<_Z$, respectively. Define $x_m(u) = x_M(b)$, $y_m(u) = y_M(g)$ and $z_m(u) = z_M(r)$, where b, g and r are the parents of u in $\mathcal{T}_1$, $\mathcal{T}_2$ and $\mathcal{T}_3$, respectively, when the parents are defined. For each special vertex v_i, $i \in \{1, 2, 3\}$, the parent is not defined in $\mathcal{T}_i$. Assign $x_m(v_1) = 0$, $y_m(v_2) = 0$ and $z_m(v_3) = 0$. For each vertex u, define a box $R(u)$ as $[x_M(u), x_m(u)] \times [y_M(u), y_m(u)] \times [z_M(u), z_m(u)]$.

The boxes defined above yield a box-contact representation for G. Similarly, a representation for the dual graph G^* is computed. These representations can be combined together; see [1] for details. Finally, the three boxes for the three outer vertices of G^* are replaced by a single shell-box, which forms the boundary of the entire representation.

The algorithm runs in $\mathcal{O}(|V|)$ time since computing the primal and the dual Schnyder woods [13], computing ordered path partitions from Schnyder woods (Lemma 1), and the computation of the coordinates all can be accomplished in linear time. $\qquad\square$

3 L-Contact Representation of Optimal 1-Planar Graphs

In this section we prove Corollary 1 and Theorem 2. Throughout, let G be an optimal 1-planar graph with a fixed 1-planar embedding. An edge is *crossing* if it crosses another edge, and *non-crossing* otherwise. A cycle in a connected graph is *separating* if removing it disconnects the graph. We list some properties of optimal 1-planar graphs.

Lemma 2 (Brinkmann et al. [8], Suzuki [22]).

- *The subgraph of an embedded optimal 1-planar graph G induced by the non-crossing edges is a plane quadrangulation Q with bipartition classes W and B.*
- *The induced subgraphs $G_W = G[W]$ and $G_B = G[B]$ on white and black vertices, respectively, are planar and dual to each other.*
- *G_B and G_W are 3-connected if and only if Q has no separating 4-cycles.*
- *There exists a simple optimal 1-planar graph with quadrangulation Q if and only if Q is 3-connected.*

An optimal 1-planar graph is *prime* if its quadrangulation has no separating 4-cycle.

Corollary 1. *Every prime 1-planar graph G has a shelled box-contact representation in 3D and it can be computed in linear time.*

Proof. Let Q be the quadrangulation of G and let B, W be the bipartition classes of Q. By Lemma 2, $G_B = G[B]$ and $G_W = G[W]$ are 3-connected planar and dual to each other. By Theorem 1, a primal-dual box-contact representation Γ of G_B can be computed in linear time. We claim that Γ, with the outer face of G_B as bounding box, is a contact representation of G. Indeed, the edges of G are partitioned into G_B, G_W, Q. Each edge in G_B is realized by contact of two "primal" boxes, each edge in G_W by contact of "dual" boxes, and each edge in Q by contact of a primal and a dual box. $\qquad\square$

(a)   (b)   (c)
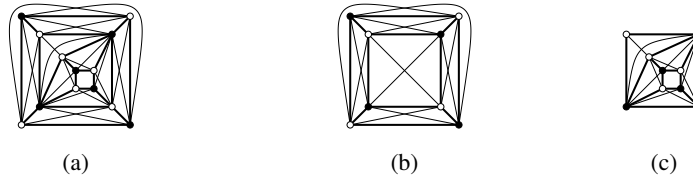
Fig. 5: (a) An embedded optimal 1-planar graph, its quadrangulation Q (bold) and the partition into white and black vertices. (b) The graph G_{out} produced by removing the interior of separating 4-cycle C. (c) The graph $G_{in}(C)$ comprised of the separating 4-cycle and its interior.

Next, assume that G is any (not necessarily prime) optimal 1-planar graph. To find an $\mathcal{L}$-representation for G, we find all separating 4-cycles in G, replace their interiors by a pair of crossing edges and construct an $\mathcal{L}$-representation Γ_{out} of the obtained prime 1-planar graph G_{out} from a shelled box-contact representation given by Corollary 1. We ensure that Γ_{out} has some "available space" where we place the $\mathcal{L}$-representations for the removed subgraph in each separating 4-cycle, which we construct recursively. We remark that similar procedures were used, e.g., for maximal planar graphs and their separating triangles [12,23]. A separating 4-cycle is *maximal* if its interior is inclusion-wise maximal. A 1-planar graph with at least 5 vertices is *almost-optimal* if its non-crossing edges induce a quadrangulation Q and inside each face of Q, other than the outer face, there is a pair of crossing edges.

Algorithm *L-Contact*(optimal 1-planar graph G)
1. Find all separating 4-cycles in the quadrangulation Q of G
2. **if** some inner vertex w of Q is adjacent to two outer vertices of Q
3.   **then** $\mathcal{C}=$ the two 4-cycles containing w and 3 outer vertices of Q. **(Case 1)**
      else $\mathcal{C}=$ set of all maximal separating 4-cycles in Q. **(Case 2)**
4. Take the optimal 1-planar (multi)graph G_{out} obtained from G by replacing for each 4-cycle $C \in \mathcal{C}$ all vertices strictly inside C by a pair of crossing edges; see Fig. 5b.
5. Compute an $\mathcal{L}$-representation of G_{out} with "some space" at each 4-cycle $C \in \mathcal{C}$. In Case 2, this is based on the box-contact representation of G_{out} in Corollary 1.
6. For each $C \in \mathcal{C}$, take the almost-optimal 1-planar subgraph $G_{in}(C)$ induced by C and all vertices inside C; see Fig. 5c. Recursively compute an $\mathcal{L}$-representation of $G_{in}(C)$ and insert into the corresponding "space" in the $\mathcal{L}$-representation of G_{out}.

Let us formalize the idea of "available space" mentioned in steps 5 and 6. Let Γ be any $\mathcal{L}$-representation of some graph G and C be a 4-cycle in G. A *frame for C* is a 3-dimensional axis-aligned box F together with an injective mapping of $V(C)$ onto the facets of F such that the two facets without a preimage are adjacent. Every frame has one of two possible types. If two opposite vertices of C are mapped onto two opposite facets of F, then F has type $(\perp-||)$; otherwise, F has type $(\perp-\perp)$; see Fig. 6b. Finally, for an almost-optimal 1-planar graph G with corresponding quadrangulation Q and outer face C, and a given frame F for C, we say that an $\mathcal{L}$-representation Γ of G *fits into F* if replacing the boxes or $\mathcal{L}$'s for the vertices in C by the corresponding facets of F yields a proper contact representation of $G - E(G[C])$ that is strictly contained in F.
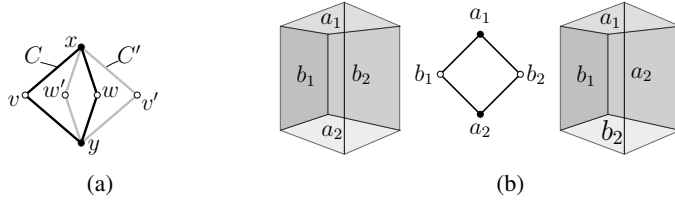
Fig. 6: (a) Illustration for Lemma 3. (b) A frame of type $(\perp - ||)$ (left) and of type $(\perp - \perp)$ (right).

Before we prove Theorem 2, we need one last lemma addressing the structure of maximal separating 4-cycles in almost-optimal 1-planar graphs.

Lemma 3. *Let G be an almost-optimal 1-planar graph with corresponding quadrangulation Q. Then all maximal separating 4-cycles of Q are interior-disjoint, unless two inner vertices w and w' of Q are adjacent to two outer vertices of Q.*

Proof. When two maximal separating 4-cycles C and C' are not interior-disjoint, then some vertex from C lies strictly inside C' and some vertex from C' lies strictly inside C. It follows that $V(C) \cap V(C')$ is a pair x, y of two vertices from the same bipartition class of Q, say $x, y \in B$, and that some $v \in V(C)$ lies strictly outside C' and some $v' \in V(C')$ lies strictly outside C. We have $v, v' \in W$ and that $C^* = (x, v, y, v')$ is a 4-cycle whose interior strictly contains C and C'. By the maximality of C and C', C^* is not separating. Since the vertices $w \in V(C) \setminus V(C^*)$ and $w' \in V(C') \setminus V(C^*)$ lie strictly inside C^*, C^* is the outer cycle of Q and w, w' are the desired vertices.   □

Theorem 2. *Every embedded optimal 1-planar graph $G = (V, E)$ has a proper $\mathcal{L}$-contact representation in 3D and it can be computed in $\mathcal{O}(|V|^2)$ time.*

Proof. Let Q be the quadrangulation of G with outer cycle C_{out}. Following algorithm **L-Contact**, we distinguish two cases. If (**Case 1**) some inner vertex w of Q has two neighbors on C_{out} we let $\mathcal{C}$ be the set of the two 4-cycles in Q that consist of w and 3 vertices of C_{out}. Otherwise (**Case 2**), let $\mathcal{C}$ be the set of all maximal separating 4-cycles in Q. By Lemma 3 the cycles in $\mathcal{C}$ are interior-disjoint. As in step 4 we define G_{out} to be the optimal 1-planar (multi)graph obtained from G by replacing for each $C \in \mathcal{C}$ all vertices strictly inside C by a pair of crossing edges. Note that in Case 1 the quadrangulation corresponding to G_{out} is $K_{2,3}$ with inner vertex w. We proceed by proving the following lemma, which corresponds to step 5 in the algorithm.

Lemma 4. *Let H be an almost-optimal 1-planar (multi)graph whose corresponding quadrangulation Q_H is either $K_{2,3}$ or has no separating 4-cycles. Let $\mathcal{C}$ be a set of facial 4-cycles of Q_H, different from its outer cycle C_o, and H' be the graph obtained from H by removing the crossing edges in each $C \in \mathcal{C}$. Then for any given frame F for C_o, one can compute an $\mathcal{L}$-representation Γ of H' fitting into F so that there is a frame $F_C \subseteq F$ for every $C \in \mathcal{C}$ that is interior-disjoint from all boxes and $\mathcal{L}$'s in Γ.*

Proof. **Case 1, $Q_H = K_{2,3}$.** Let w be the inner vertex of H. Without loss of generality let $F = [0,5] \times [0,5] \times [0,4]$ and let $V(C_o)$ be mapped onto the top, back left, bottom
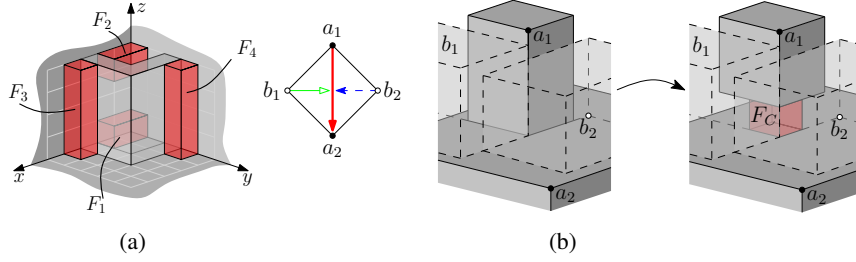
Fig. 7: Illustration for Lemma 4: (a) Case 1 construction, (b) Creating a frame F_C in Case 2 for an inner facial cycle $C = (a_1, b_1, a_2, b_2)$ of Q_H by releasing the contact between a_1 and a_2.

and back right facets of F. Define the $\mathcal{L}$ for w to be the union of $[0,3] \times [2,3] \times [0,4]$ and $[2,3] \times [0,3] \times [0,4]$. Define four boxes $F_1 = [0,2] \times [0,1] \times [0,1]$, $F_2 = [0,2] \times [0,1] \times [3,4]$, $F_3 = [3,4] \times [0,1] \times [0,4]$ and $F_4 = [0,1] \times [3,4] \times [0,4]$, each completely contained in F and disjoint from the $\mathcal{L}$ for w; see Fig. 7a. Each F_i, $i \in \{1,2,3,4\}$ is a frame for a 4-tuple containing w and three vertices of C_o. Thus independent of the type of F and the neighbors of w in Q_H, we find a frame for the inner faces of Q_H.

Case 2, $Q_H \neq K_{2,3}$. Let B and W be the bipartition classes of Q_H and $C_o = (v_1, w_1, v_2, w_2)$ with $v_i \in B$ and $w_i \in W$, $i = 1, 2$. Without loss of generality v_1, v_2, w_1 are mapped onto the back left, back right and top facets of F, respectively, and w_2 is mapped onto the bottom facet if (**Case 2.1**) F has type $(\perp-||)$ and onto the front left facet if (**Case 2.2**) F has type $(\perp-\perp)$. Let H^* be the graph obtained from H by inserting a pair of crossing edges in C_o, leaving v_1, w_2 and v_2 on the unbounded region. By assumption, H^* is a prime 1-planar graph and thus by Lemma 2 $H_B^* = H^*[B]$ and $H_W^* = H^*[W]$ are planar 3-connected and dual to each other. We choose v_3 to be the clockwise next vertex after v_2 on the outer face of H_B^* and compute (using Corollary 1) a shelled box-contact representation Γ^* of H^*, in which w_2 is represented as the bounding box $F^* = [0,n]^3$, $n \in \mathbb{N}$, and v_1, v_2, w_1 as $[0,n] \times [0,1] \times [0,n]$, $[0,1] \times [0,n] \times [1,n] \times [1,n] \times [n-1,n]$, i.e., these boxes constitute the back left, back right and top facets of F^*, respectively.

Next we show how to create a frame for each facial 4-cycle $C \in \mathcal{C}$. Let a_1, b_1, a_2, b_2 be the vertices of C in cyclic order. Assume without loss of generality that $a_1, a_2 \in W$ and $b_1, b_2 \in B$. Thus (a_1, a_2) and (b_1, b_2) are crossing edges of H_W^* and H_B^*, respectively. In the Schnyder wood of H_W^* underlying Corollary 1 exactly one of (a_1, a_2), (b_1, b_2) is uni-directed, say (a_1, a_2) is uni-directed in tree $\mathcal{T}_1$. Then there is a point in $\mathbb{R}^3$ in common with all four boxes in Γ^* corresponding to vertices of C. Moreover, by construction boxes b_1, a_2, b_2 touch box a_1 with their y^+, z^+, y^- facets, respectively; see Fig. 7b. Now we can increase the lower z-coordinate of the box a_1 by some $\varepsilon > 0$ so that a_1 and a_2 lose contact and between these two boxes a cubic frame F_C with side length ε is created; see again Fig. 7b. Note that the z^- facet of a_1 makes contact only with a_2 and hence if ε is small enough all other contacts in Γ^* are maintained. We apply this operation to each $C \in \mathcal{C}$ and obtain a shelled box-representation Γ' of H'.

Finally, we show how to modify Γ' to obtain an $\mathcal{L}$-representation of H' fitting the given frame F. If (**Case 2.1**) F has type $(\perp-||)$, we define a new box for w_2 to be
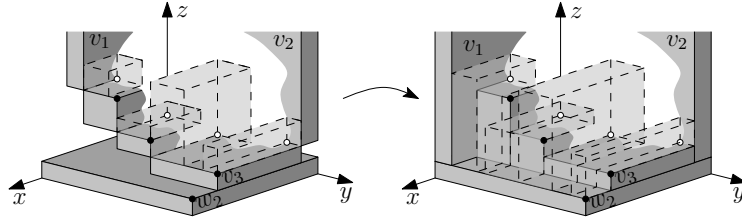
Fig. 8: Modifying Γ' when F has type $(\perp-||)$ (Case 2.1) to find a representation fitting F.

$[0, n+1] \times [0, n] \times [-1, 0]$. For each white neighbor of w_2 we union the corresponding box with another box that is contained in $[n, n+1] \times [0, n] \times [0, n]$ with bottom facet at $z = 0$ so that the result is an $\mathcal{L}$-shape. For each black neighbor of w_2 we set the lower z-coordinate of the corresponding box to 0; see Fig. 8. (This requires the proper contacts for outer edges of G_B, except for (v_1, v_2), to be parallel to the xz-plane, which we can easily guarantee.) We then apply an affine transformation mapping $[1, n+1] \times [1, n] \times [0, n-1]$ onto F. If (**Case 2.2**) F has type $(\perp-\perp)$, define a new box for w_2 to be $[0, n] \times [n, n+1] \times [0, n]$ and apply an affine transformation mapping $[1, n] \times [1, n] \times [0, n-1]$ to F. In both cases we have an $\mathcal{L}$-representation of H' fitting F. □

By the lemma above we can compute an $\mathcal{L}$-representation Γ_{out} of G_{out} fitting any given frame F_{out} for C_{out} in $\mathcal{O}(|V(G_{out})|)$ time. Moreover, Γ_{out} has a set of disjoint frames $\{F_C \mid C \in \mathcal{C}\}$. Following step 6 of algorithm **L-Contact**, for each $C \in \mathcal{C}$, let $G_{in}(C)$ be the almost-optimal 1-planar graph given by all vertices and edges of G on and strictly inside C. Recursively applying the lemma we can compute an $\mathcal{L}$-representation Γ_C of $G_{in}(C)$ fitting the frame F_C for C in Γ_{out}. Clearly, $\Gamma = \Gamma_{out} \cup \bigcup_{C \in \mathcal{C}} \Gamma_C$ is an $\mathcal{L}$-representation of G fitting F_{out}. We pick a frame F_{out} of arbitrary type for C_{out} to complete the construction. Although computing an $\mathcal{L}$-representation of G_{out} takes $\mathcal{O}(|V(G_{out})|)$ time, recursive computation and affine transformations on the $\mathcal{L}$'s for the vertices in $G_{in}(C)$ for each $C \in \mathcal{C}$ require $\mathcal{O}(|V|^2)$ time. □

4 Conclusion and Open Questions

We described efficient algorithms for 3D contact representation of several types on non-planar graphs. Many interesting problems remain open. A planar graph has a contact representation with rectangles in 2D if and only if it has no separating triangles. Is there a similar characterization for 3D box-contact representations? It is known that any planar graph admits a proper contact representation with boxes in 3D and a non-proper contact representation with cubes (boxes with equal sides). Does every planar graph admit a proper contact representation with cubes? Representing graphs with contacts of constant-complexity 3D shapes, such as $\mathcal{L}$'s, is open for many graph classes with a linear number of edges, such as 1-planar, quasi-planar and other nearly planar graphs.

References

1. Alam, M.J., Evans, W.S., Kobourov, S.G., Pupyrev, S., Toeniskoetter, J., Ueckerdt, T.: Contact representations of graphs in 3D. CoRR abs/1501.00304 (2015)
2. Andreev, E.: On convex polyhedra in Lobachevskii spaces. Mat. Sb. 123(3), 445–478 (1970)
3. Badent, M., Brandes, U., Cornelsen, S.: More canonical ordering. Journal of Graph Algorithms and Applications 15(1), 97–126 (2011)
4. Bernardi, O., Fusy, E.: Schnyder decompositions for regular plane graphs and application to drawing. Algorithmica 62(3–4), 1159–1197 (2012)
5. Bezdek, A.: On the number of mutually touching cylinders. Combinatorial and Computational Geometry 52, 121–127 (2005)
6. Bonichon, N., Felsner, S., Mosbah, M.: Convex drawings of 3-connected plane graphs. Algorithmica 47(4), 399–420 (2007)
7. Bremner, D., Evans, W., Frati, F., Heyer, L., Kobourov, S., Lenhart, W., Liotta, G., Rappaport, D., Whitesides, S.: Representing graphs by touching cuboids. In: Graph Drawing. LNCS, vol. 7704, pp. 187–198. Springer (2013)
8. Brinkmann, G., Greenberg, S., Greenhill, C., McKay, B., Thomas, R., Wollan, P.: Generation of simple quadrangulations of the sphere. Discrete Math. 305(1–3), 33–54 (2005)
9. Buchsbaum, A.L., Gansner, E.R., Procopiuc, C.M., Venkatasubramanian, S.: Rectangular layouts and contact graphs. ACM Transactions on Algorithms 4(1) (2008)
10. Czyzowicz, J., Kranakis, E., Urrutia, J.: A simple proof of the representation of bipartite planar graphs as the contact graphs of orthogonal straight line segments. Information Processing Letters 66(3), 125–126 (1998)
11. Fabrici, I., Madaras, T.: The structure of 1-planar graphs. Discrete Mathematics 307(7–8), 854–865 (2007)
12. Felsner, S., Francis, M.C.: Contact representations of planar graphs with cubes. In: Hurtado, F., van Kreveld, M.J. (eds.) SOCG. pp. 315–320. ACM (2011)
13. Felsner, S., Zickfeld, F.: Schnyder woods and orthogonal surfaces. Discrete & Computational Geometry 40(1), 103–126 (2008)
14. de Fraysseix, H., de Mendez, P.O.: Representations by contact and intersection of segments. Algorithmica 47(4), 453–463 (2007)
15. Gonçalves, D., Lévêque, B., Pinlou, A.: Triangle contact representations and duality. Discrete & Computational Geometry 48(1), 239–254 (2012)
16. Hliněný, P., Kratochvíl, J.: Representing graphs by disks and balls (a survey of recognition-complexity results). Discrete Mathematics 229(1–3), 101–124 (2001)
17. Kobourov, S.G., Ueckerdt, T., Verbeek, K.: Combinatorial and geometric properties of planar Laman graphs. In: Khanna, S. (ed.) SODA. pp. 1668–1678. SIAM (2013)
18. Koebe, P.: Kontaktprobleme der konformen Abbildung. Berichte über die Verhandlungen der Sächsischen Akad. der Wissen. zu Leipzig. Math.-Phys. Klasse 88, 141–164 (1936)
19. Mohar, B.: Circle packings of maps in polynomial time. European Journal of Combinatorics 18(7), 785–805 (1997)
20. Ringel, G.: Ein Sechsfarbenproblem auf der Kugel. Abhandlungen aus dem Mathematischen Seminar der Universitat Hamburg 29(1–2), 107–117 (1965)
21. Schumacher, H.: Zur struktur 1-planarer graphen. Math. Nachrichten 125, 291–300 (1986)
22. Suzuki, Y.: Re-embeddings of maximum 1-planar graphs. SIAM Journal on Discrete Mathematics 24(4), 1527–1540 (2010)
23. Thomassen, C.: Interval representations of planar graphs. Journal of Combinatorial Theory Series B 40(1), 9–20 (1988)